

Phase and microstructure evolution during solidification of Nd-Fe-B melts processed by novel techniques

O. FILIP*, R. HERMANN^a

Department of Material Science 6, University of Erlangen-Nurnberg, Martensstr. 7, D-91058 Erlangen, Germany

^aLeibniz Institute for Solid State and Materials Research (IFW) Dresden, P.O. Box 270016, D-01171 Dresden, Germany

The influence of different techniques and process parameters like the cooling rate, undercooling level and melt convection on the phase and microstructure selection during the solidification process of stoichiometric Nd₂Fe₁₄B melts is discussed. Using an electromagnetic levitation technique, in-situ observation of the solidification kinetics was performed. Small additions of Ti and C were found to decrease significantly the growth rate of the Nd₂Fe₁₄B phase in the undercooled stages. Comparing with the stoichiometric Nd₂Fe₁₄B melt, here, only moderate quenching rates are necessary in order to suppress the formation of large unconsumed α -Fe dendrites. The microstructure formation appears to be strongly related with the precipitation mechanism of fine TiC particles during thermal processing of the melt prior to quenching on chill substrates. Additionally, an important change in the volume fraction and grain size of the residual α -Fe phase was observed to be produced by different melt motions at the crystallization front. A distinct reduction of the amount of α -Fe was measured in samples which were subjected to strong rotation in levitation, during the cooling process. A prove that the microstructure formation during the solidification process can be controlled by enhancement or suppression of the melt convection was given employing a specially designed forced crucible rotation/vibration technique.

(Received January 18, 2006; accepted March 23, 2006)

Keywords: Nd-Fe-B magnets, Undercooled melts, Growth kinetics, Melt convection

1. Introduction

From its discovery, Nd-Fe-B material has attracted enormous attention in the scientific and industrial world, proving to be an economically successful magnetic material. Its rapid development in industrial applications is due to the excellent intrinsic magnetic properties of the Nd₂Fe₁₄B (Φ) phase [1]. The high saturation magnetization and the high anisotropic field provided by the hard magnetic Φ phase represent only an excellent prerequisite in order to obtain high energy Nd-Fe-B magnets. Good extrinsic magnetic properties of the final permanent magnet are derived from the intrinsic properties by the preparation of an adequate microstructure. The ability to control the microstructure formation during the solidification process is the key to the development of favourable microstructure. The suppression of the α -Fe phase which forms due to an incomplete peritectic reaction during the solidification process of Nd-Fe-B alloys, deteriorating the coercive field of the permanent magnet, is of interest for the production of near stoichiometric compounds. Containerless electromagnetic levitation technique is useful to achieve substantial undercooling of metallic melts, avoiding heterogeneous nucleation at the crucible wall [2]. Using this processing technique, in-situ temperature-time measurements allow the detailed study of the recalescence event in the undercooled stage. Quenching experiments by dropping the

electromagnetically levitated samples at different undercooling levels onto chill substrates revealed that the phase selection in the Nd-Fe-B materials is strongly dependent on the undercooling level prior to solidification [3]. Small additions of Ti and C or Mo were found to change importantly the solidification kinetics in these alloys [4,5]. Besides the influence of thermal processing of the melts prior to quenching and melt composition, forced melt convection externally induced by electromagnetic fields was found to play a crucial role on the microstructure formation [6,7]. The aim of this work is to investigate the role of Ti and C additions on the solidification process of rapidly quenched Nd-Fe-B-Ti-C samples. Additionally, the microstructure evolution, mainly the volume fraction of the soft magnetic α -Fe phase, in consideration of forced enhancement or suppression of melt convection has been experimentally investigated with a specially designed crucible rotation/vibration technique.

2. Experimental

Different compositions of (Nd₂Fe₁₄B)_{100-2x}Ti_xC_x alloys (x = 0; 0.5; 1; 3) were prepared by induction melting of pure elements of Nd (99.9%), Fe (99.9%), Ti (99.9%) and 80Fe20C and 45Fe55B pre-alloys. Samples with a mass of about 1.5 g were prepared for the electromagnetic levitation experiments. The levitation of the samples is

facilitated by an oscillating magnetic field which is produced by an applied RF-alternating current on a cone-like induction coil. Eddy currents are induced in conductive samples where the magnetic force compensates the gravitational force. Additionally, the sample is melted by the absorbed power. The molten samples were cooled by a gas stream with different cooling rates (2 - 60 K/s). The small levitated droplets were repeatedly melted, overheated and then cooled with different cooling rates up to spontaneous solidification in undercooled state. The growth velocity of the solidification front was determined by revealing the recalescence step of the in-situ recorded temperature-time characteristics. The temperature was measured at the top of the sample employing a two-colour pyrometer. Also, the solidification event was monitored from the side, using a fast responding silicon photo diode with a sampling rate of 1MHz. In intentionally selected cases, at different undercooling levels, the samples were quenched during cooling onto tin-coated copper substrates. The microstructure formation in a cross-section of the quenched samples was investigated by electron (SEM) and optical (Kerr) microscopy. For the spontaneously solidified samples, additional to the levitated droplets, samples which were fixed at the bottom side on a boron nitride (BN) plate, thus inhibiting global sample rotation (which unavoidably occurs in levitated samples), were investigated. The experiments where the molten alloys were subjected to forced rotation/vibration movements with defined rates up to about 250 Hz were performed in especially built apparatus. The samples were sealed in quartz ampoules of different diameters under 700 mbar argon atmosphere, and fixed in a quartz tube. The whole arrangement was placed perpendicular on an AC motor and centred in an induction coil. In differently solidified samples the volume fraction of α -Fe was determined using a vibrating sample magnetometer (VSM). The samples were crushed to powder and sieved. Particle size fractions of 350 to 500 μm were selected and magnetically investigated. Assuming that only two magnetic phases, α -Fe and $\text{Nd}_2\text{Fe}_{14}\text{B}$ phase exist, the magnetic measurements were carried out at 340 °C, well above the Curie temperature of the $\text{Nd}_2\text{Fe}_{14}\text{B}$ phase, in up to 1.5 T magnetic field strength under argon atmosphere.

3. Results and discussion

3.1 Growth kinetics

The samples were overheated in electromagnetic levitation up to a temperature of about 1600 °C and then cooled by a He-gas stream. The solidification occurred spontaneously at undercooling levels which amounted to 30-250 K below the liquidus temperature. The growth velocity of the $\text{Nd}_2\text{Fe}_{14}\text{B}$ phase was estimated from the crossing time of the solidification front through the viewing field of the pyrometer and the diode, respectively, assuming a planar solidification front. Fig. 1 shows the dependence of the growth velocity on the undercooling level of a stoichiometric Nd-Fe-B alloy without and with Ti and C additions. The growth rate increases with

increasing undercooling for all compositions. A difference appears at high undercooling levels where the growth velocity in the alloys with Ti and C additions is strongly reduced compared to the composition without additions. It is obvious that these additions inhibit the proceeding of the solidification front. A change in the solidification process can be understood considering that the ternary composition $\text{Nd}_2\text{Fe}_{14}\text{B}$ is a line compound and the additional alloying elements (Ti and C) change it to a solid solution. In this case, the composition of the solid is different from that of the liquid with which it is in equilibrium. This results in a build-up of a compositional gradient ahead of the solidification front. The gradient must equilibrate by diffusion before the front can advance. This mechanism reduces the growth velocity of the solidification front and is referred to as solute drag. Moreover, the undercoolability of the Nd-Fe-B-Ti-C alloys was found to be influenced by the amount of Ti and C additions as well as by the cooling rate prior to the solidification. The influence of the cooling rate on the maximum undercooling level is presented in Fig. 2. The maximum undercooling level is constant and does not depend on the cooling rate in the composition range from 0-2 at.% ($x = 0; 1$) Ti and C but it decreases slightly with increasing concentration. A drastic change is visible in the case of the composition with 6 at.% ($x = 3$) Ti and C. Here, the undercoolability increases steadily with increasing cooling rate up to a critical cooling rate of about 15 K/s. At high amount of Ti and C, the TiC precipitation phenomenon which strongly depends on the processing route prior to the solidification [8], plays an important role during the solidification of the competing phases.

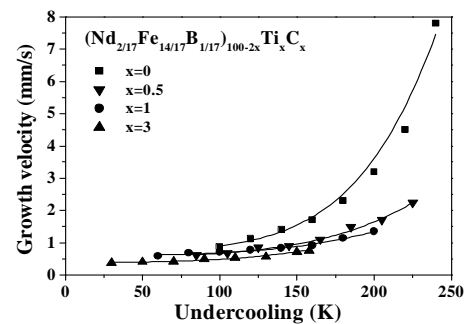


Fig. 1. Growth velocity of the solidification front vs. undercooling level.

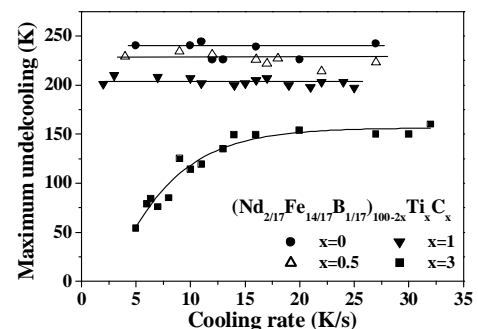


Fig. 2. Maximum undercooling level vs. cooling rate.

3.2 Microstructure formation

The microstructure of the as-solidified stoichiometric Nd-Fe-B alloy is determined by a competitive growth of the γ -Fe and the $\text{Nd}_2\text{Fe}_{14}\text{B}$ phase. Previous results given by Hermann et al. [9] showed that, at distinct undercooling levels, the spontaneous solidification of stoichiometric $\text{Nd}_2\text{Fe}_{14}\text{B}$ without additions is caused by the peritectic reaction of the $\text{Nd}_2\text{Fe}_{14}\text{B}$ phase. But quenching of the sample onto a chill substrate may lead to a modified phase selection and heterogeneous nucleation of the $\text{Nd}_2\text{Fe}_{14}\text{B}$ phase starting at the substrate side is preferred.

In order to elucidate the role of the Ti and C additions in the solidification process and microstructure formation, a series of experiments of the samples with high amount of Ti and C ($(\text{Nd}_{2/17}\text{Fe}_{14/17}\text{B}_{1/17})_{100-2x}\text{Ti}_x\text{C}_x$ ($x = 3$)) were performed. A first set of experiments consisted of samples which were strongly overheated (1873 K) above the melting point and then cooled with different cooling rates prior to the spontaneous solidification. For comparison, samples which spontaneously solidified in levitation at a temperature of about 1473 K, slightly above the melting point of the investigated alloy, were selected.

The cross-section SEM micrographs of the samples which were cooled with cooling rates of about 2 and 20 K/s, respectively, are shown in Fig. 3. A common sequence which consist of a mixture of α -Fe phase (dark gray), Nd-rich phase (white) and $\text{Nd}_2\text{Fe}_{14}\text{B}$ phase (light gray) occurs in all differently processed alloys. Characteristic for this alloy composition is the TiC phase (black) which appears in different morphologies, depending on the processing parameters. Compact TiC precipitates with cubic morphology and a large amount of pro-peritectic γ -Fe (dark grey area) dendrites develop in the microstructure within the range of low cooling rates (~ 2 K/s, Fig. 3a). The growth of the TiC precipitates is drastically reduced at higher cooling rates starting from the overheated state. Refined TiC precipitates with a dendritic structure form at about 20 K/s cooling rate, visible in Fig. 3b. It should be remarked that the nucleation of the pro-peritectic γ -Fe is affected by a strong interaction with the TiC dendrites. The TiC dendrites are completely embedded in α -Fe. At much higher cooling rates (about 60 K/s) only very small TiC particles with a size up to 3 μm were observed in the microstructure of the solidified samples. From this set of experiments, it can be concluded that TiC precipitates form already in the overheated states of the Nd-Fe-B-Ti-C melt well above the liquidus temperature, when the solubility of these elements in the molten samples is exceeded during cooling. The growth morphology of the TiC particles during the precipitation process in heated states above the melting point, changes strongly with increasing cooling rate prior to quenching. A refinement of TiC particles occurs increasing the cooling rate. Owing to the peritectic nature of the solidification sequence of the stoichiometric $\text{Nd}_2\text{Fe}_{14}\text{B}$ compound, pro-peritectic γ -Fe forms primarily at low undercooling levels. A strong interaction of the γ -Fe formation and the TiC precipitation sets if a critical cooling rate prior to quenching is exceeded. A distinct refinement of the γ -Fe

nuclei is produced, facilitating the peritectic transformation which is governed by solid phase diffusion processes. Less α -Fe remains, therefore, unconsumed in the solidified microstructure at high cooling rates.

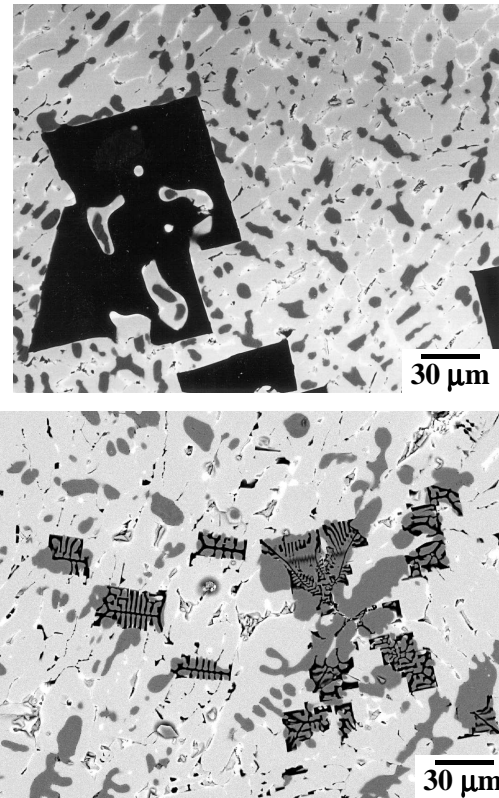


Fig. 3. SEM micrographs of $(\text{Nd}_{2/17}\text{Fe}_{14/17}\text{B}_{1/17})_{100-2x}\text{Ti}_x\text{C}_x$ ($x = 3$) samples quenched from 1473 K after cooling from 1873 K with a cooling rate of about: a) 2 K/s; b) 20 K/s.

In order to increase further the cooling rate, the samples were quenched onto chill substrates. In this set of experiments, the influence of the cooling rate of the molten sample prior to quenching on the solidification behaviour of the $(\text{Nd}_{2/17}\text{Fe}_{14/17}\text{B}_{1/17})_{94}\text{Ti}_3\text{C}_3$ samples is investigated. The samples are heated in levitation up to 1873 K and then cooled with different cooling rates to the liquidus temperature 1473 K and subsequently quenched onto tin-coated copper substrates. The cooling rates are chosen from about 2 K/s to the superior limit of about 60 K/s obtainable with the electromagnetic levitation technique.

SEM micrographs of the cross-sections of quenched samples are shown in Fig. 4. All quenched samples showed an almost featureless region at the substrate side (bottom side) corresponding (by EDX investigations) to the stoichiometric $\text{Nd}_2\text{Fe}_{14}\text{B}$ compound, caused by heterogeneous nucleation of the $\text{Nd}_2\text{Fe}_{14}\text{B}$ phase. At low cooling rates the uniform featureless layer at the substrate side has a thickness of about 500 μm (Fig. 4a). This layer is followed by a finely structured area containing α -Fe

dendrites. It extends to the opposite side (top) of the disk-like sample with a mean total thickness of about 1 mm. The layer thickness changes if the sample is cooled with a high cooling rate (60 K/s) prior to quenching (Fig. 4b). The single-phase Nd₂Fe₁₄B layer at the substrate side increases partially up to 800 μm. Moreover, at high cooling rates, a strong refinement of the α-Fe dendrites in the upper layer of the as-quenched microstructures was observed. The effect of reducing the amount of α-Fe with increasing the cooling rate prior to quenching can be explained considering the TiC precipitation phenomenon. The non-equilibrium solubility of Ti and C in the melt depends strongly on the cooling rate prior to solidification and generates at high cooling rates a much stronger solute gradient ahead of the solidification front. This fact leads to a further decrease of the growth velocity of the solidification front in undercooled samples. It results in a considerable decrease of the rate of the crystallization heat which must be removed from the solidifying system during the quenching process. In this way, at high cooling rates prior to quenching, the temperature of the solidification front remains low enough in the undercooled state for a longer period of time, promoting direct crystallisation of 2-14-1 phase in a larger volume fraction at the substrate side of the quenched sample. On the other hand, a stronger solute gradient ahead of the solidification front promotes the precipitation of the TiC particles in the vicinity of the crystallisation front. An increased number of TiC particles provides more heterogeneous nucleation sites, increasing drastically the nucleation rate of the solid phase. This can explain the strong refinement of the α-Fe dendrites in the upper part of the quenched samples which were cooled at higher rates prior to quenching.

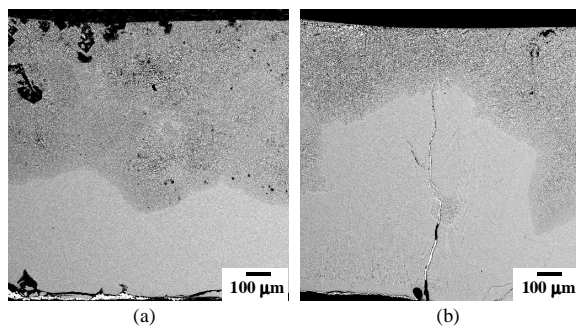


Fig. 4. SEM micrographs of $(Nd_{2/17}Fe_{14/17}B_{1/17})_{94}Ti_3C_3$ samples quenched from 1473 K after cooling from 1873 K with a cooling rate of about: a) 2 K/s; b) 60 K/s.

3.3 Influence of the melt convection on the microstructure formation

Besides the influence of the thermal processing prior to quenching on the microstructure formation in Nd-Fe-B alloys, the sample motion (rotation/vibration) which inevitably occurs during the levitation process was found to play an important role on the amount and morphology

of the unconsumed Fe during the solidification process. The electromagnetic levitation technique, has been used in order to investigate the influence of the melt rotation and turbulence on the microstructure formation of stoichiometric Nd₂Fe₁₄B alloys, mainly the volume fraction and grain size of the undesired α-Fe phase. Convection modes driving the melt motion are the electromagnetically driven convection, heat diffusion, buoyancy and the Marangoni convection. On the other hand, the free sample levitation enforces a strong sample rotation with about 10 Hz frequency which superposes the primary convection modes. The effect of the sample rotation on the internal melt flow was studied numerically and details are described elsewhere [10]. The basic flow Reynolds number of the internal melt flow and especially under global melt rotation has been demonstrated using the Ekman number E which describes the ratio of viscous force and Coriolis force. It could be shown that higher rotation rates corresponding to $E < 10^{-2}$ may drastically reduce the internal motion. Hereby, the characteristic

Ekman number is expressed by $E = \frac{\nu}{\Omega R^2}$, where ν

denotes the kinematic viscosity of the melt, R the radius of the ampoule and $\Omega = 2\pi f$ the global rotation. The interpretation is that a high-speed rotation forces the fluid to rotate more and more as a solid body, thus suppressing the relative internal motion like in a centrifuge. That means, compared to the non-rotating case the global melt rotation suppresses the internal melt motion significantly by about two orders of magnitude. To compare, samples solidified in static conditions were produced touching the sample bottom on a BN plate which inhibited the global sample rotation. The samples were cooled by a He gas stream till the onset of the spontaneous solidification or the triggered solidification at distinct undercooling levels. These two different solidification procedures were additionally modified by applying different cooling rates (2 and 18 K/s, respectively).

A: constant undercooling level and varying cooling rate

Fig. 5a and 5b show the SEM micrographs of samples which were slowly cooled up to the spontaneous solidification at about 40 K below the liquidus temperature. Hereby, sample 1 (Fig. 5a) was levitated, causing strong sample rotations whereas sample 2 (Fig. 5b) was processed without rotations by fixing the sample on a BN plate. It is clearly obvious that the α-Fe dendrites appear much larger in sample 2. The α-Fe volume fraction was determined by measuring the magnetic moment of the sample at 340 °C in a magnetic field of 1.5 T yielding approximately the double α-Fe fraction for the samples without additional rotation. Beyond it, high cooling rates prior to the solidification lead to further α-Fe dendrite refinement with slight reduction of the α-Fe volume fraction. The results of the determined α-Fe volume fraction are listed in Table 1. For this sample set, the undercooling level of 50 K was justified as a constant parameter. It can be established that the strong sample rotation superposing the internal melt convection

diminishes the α -Fe volume fraction as well as the α -dendrite dimension drastically.

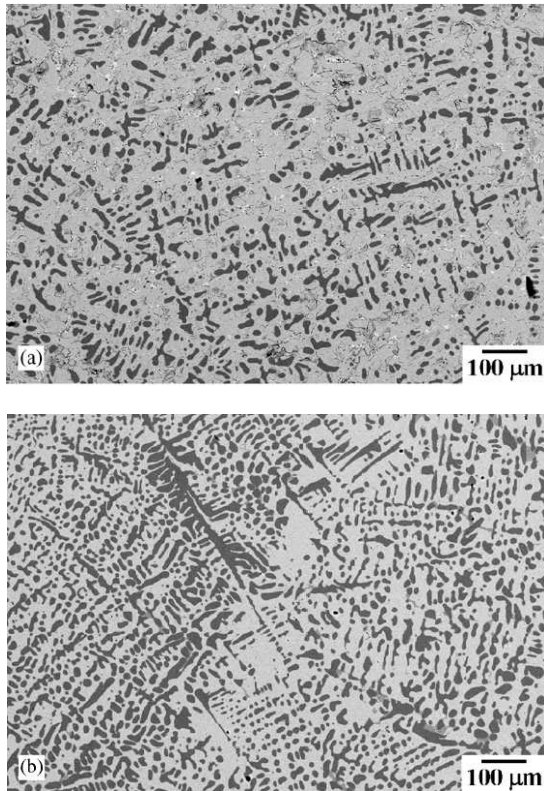


Fig. 5. SEM micrographs of samples cooled with a cooling rate of 2 K/s to about 50 K below the liquidus temperature prior to solidification: (a) sample processing in levitation, (b) sample processing on a BN plate.

Table 1. α -Fe volume fraction measured with VSM.

	α -Fe volume fraction (wt%)
Sample 1-slow cooling rate/levitation	15
Sample 2-slow cooling rate/BN plate	28
Sample 3-high cooling rate/levitation	13
Sample 4-high cooling rate/BN plate	25

B: constant undercooling rate and varying undercooling level

A second experimental set was conducted for the investigation of the undercooling level prior to solidification and the microstructure development. The samples could be undercooled up to 170 K below the

liquidus temperature with a constant cooling rate of 15 K/s. The graphical presentation in Fig. 6 provides a concise overview about the measured α -Fe volume fraction in levitated samples and on BN plate fixed samples in dependence on the undercooling level. It is again clearly visible that the α -Fe volume fraction in levitated samples with strong sample rotation amounts to distinct lower values than in the fixed samples. Thereby the α -Fe volume fraction seems to increase with undercooling for the fixed samples whereas it roughly levels off in the strongly rotating samples, but the few points with comparable parameters which were selected from numerous experiments do not allow a precise description of this fact. It is important to look at the proportion of the measured values in one experiment and the tendency which it points out. The observation of the full cross-section of the sample hemispheres permits the study of the homogeneity of the α -Fe phase distribution. Strong sample rotation supports a homogeneous α -Fe dendrite formation whereas sometimes a quite inhomogeneous microstructure has been observed in samples which were processed on the BN plate. The grain size of the solidified samples was investigated by KERR microscopy. A grain refinement during solidification under strong sample rotation could be detected. The reduction of the α -Fe volume fraction and the grain refinement is hard to explain without any additional numerical treatment which is the strategy for future work. The sample rotation superposed the internal melt convection seems to retard rapid dendrite growth. The fine structured Fe dendrites provide numerous nucleation centres for the succeeding solidification of the residual melt, the peritectic growth of the $\text{Nd}_2\text{Fe}_{14}\text{B}$ phase from properitectic α -Fe and the surrounding melt resulting in reduced grain growth.

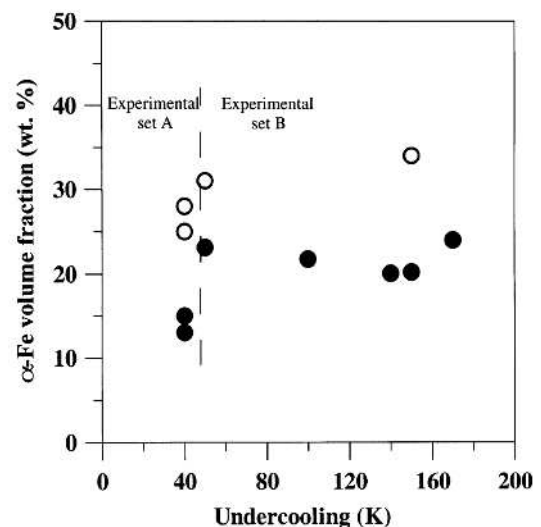


Fig. 6. α -Fe volume fraction determined with VSM vs. undercooling: (a) filled circle - sample processing in levitation, (b) open circle - sample processing on a BN plate.

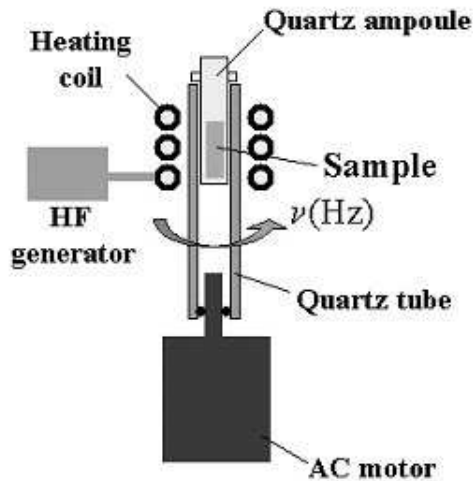


Fig. 7. Experimental arrangement for forced melt rotation.

Table 2. α -Fe – volume fraction in dependence on the rotation frequency (rpm) for $\varnothing 6$ mm – samples and $\varnothing 18$ mm – samples, stoichiometric composition.

	example 1 $\varnothing 6$ mm	example 2 $\varnothing 6$ mm	example 3 $\varnothing 6$ mm
f (rpm)	100	500	2500
α -Fe (wt-%)	24.40	22.57	18.80
		example 4 $\varnothing 18$ mm	example 5 $\varnothing 18$ mm
f (rpm)		55.5	278
α -Fe (wt-%)		21.88	18.54

In order to prove that the microstructure formation during the solidification process can be controlled by enhancement or suppression of the melt convection by forced sample rotation, a special apparatus has been built. The arrangement is schematically shown in Fig. 7. The experiments with the stoichiometric compound $\text{Nd}_2\text{Fe}_{14}\text{B}$ yielded a drastic reduction of the α -Fe-phase volume fraction which deteriorates the hard magnetic properties, under strong global melt rotation during solidification deducing a reduced growth of α -Fe-nuclei at suppressed internal fluid flow. The α -Fe volume fraction dropped with increasing global melt rotation at about 25% with rising rotation rates from 100 rpm up to about 2500 rpm (Fig. 8). For a possible industrial application of the forced rotation technique during solidification of peritectic Nd-Fe-B alloys, it is worth to prove the availability to large crucibles. Therefore, experiments with extended

diameters were performed. As mentioned above, the correlation between the cylindrical sample volume and the rotation frequency is described by E and follows

$$f = \frac{v}{2\pi ER^2} \quad (1)$$

Starting from the assumption of equal fluid flow state in samples with different diameters according to similar microstructure and phase distribution, the resulting rotation frequency as main parameter can be calculated from equation (1). Samples with 6 mm diameter and the threefold diameter of 18 mm have been prepared. Using the highest possible frequency of 2500 rpm and a medium frequency of 500 rpm, respectively for the 6 mm ampoule, the relating frequencies for the 18 mm ampoule amount to 278 rpm and 55.5 rpm, respectively. The α -Fe volume fractions determined by VSM are summarised in Table 2. It is clearly visible that indeed the comparable examples 2 and 4 as well as 3 and 5 yield approximately the same α -Fe volume fraction. This dependence is additionally shown in Fig. 8. Because rotation frequency and sample diameter are reciprocally proportional, a very good industrial relevance can be expected going to large sample dimensions. Characteristic cross sections of the samples were investigated with scanning electron microscopy. The sample with 100 rpm rotation frequency displays larger α -Fe phase fraction than the sample processed with 2500 rpm rotation frequency corresponding to reduced internal melt flow.

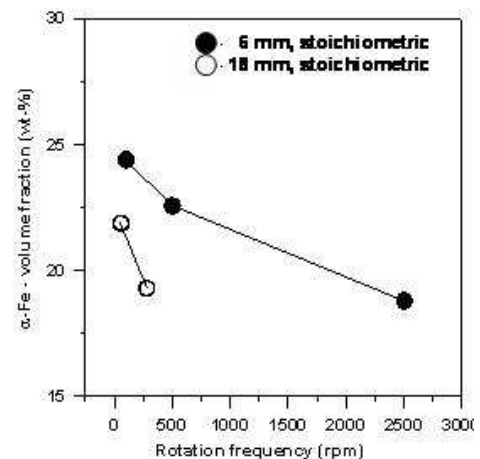


Fig. 8. α -Fe volume fraction in dependence on the rotation frequency and sample diameter.

An additional proof for the correlation between internal melt flow and the growth of the peritectic α -Fe volume fraction has been done by a modified experimental arrangement. Hereby, the continuous rotation of the ampoule was changed into a bi-directional drive leading to a shaking of the melt with a strong enhanced melt motion. The graphic plot in Fig. 9 represents the strong increase of the α -Fe volume fraction with rising shaking frequency compared to the reduced α -Fe volume fraction under reduced internal motion.

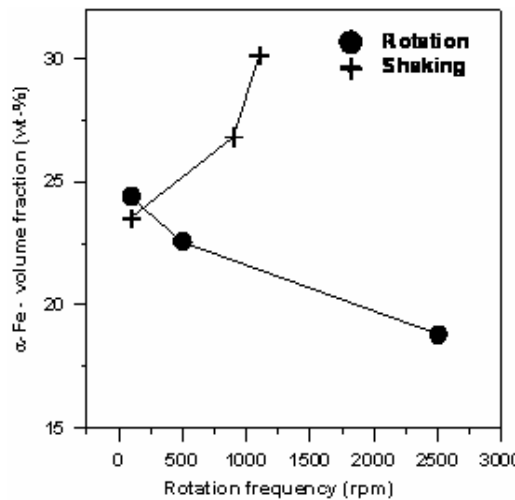


Fig. 9. α -Fe volume fraction in dependence on the rotation frequency for unidirectional rotation and shaking of the melt, stoichiometric composition and 6 mm sample diameter.

The application of a magnetic field on an electrically conducting melt during solidification offers the opportunity to much stronger influence on the fluid flow. With the construction of a special magnetic two-phase stirrer design we provided the basis for the well designed contactless influence on the melt motion [11]. Further work will be done using additional magnetic fields.

4. Conclusions

Using the containerless electromagnetic levitation technique, small samples with a mass up to 1.5 g are deeply undercooled till the onset of the spontaneous solidification. The growth velocity increases moderately with increasing undercooling in Nd-Fe-B-Ti-C alloys, in comparison to the stoichiometric $\text{Nd}_2\text{Fe}_{14}\text{B}$ compound where the velocity increases from 1 to 8 mm/s at a maximum achieved undercooling of about 235 K. At high undercooling levels, the growth velocity is strongly reduced in samples with Ti and C additions. It is obvious that these additions inhibit the proceeding of the solidification front. The growth of the TiC precipitates is drastically retarded, when the cooling rate is increased. The nucleation of the pro-peritectic γ -Fe is affected by a strong interaction with the TiC dendrites depending on the cooling rate. A remarkable reduction of the α -Fe volume fraction in the quenched samples with Ti and C additions is obtained. The investigations of the Nd-Fe-B-Ti-C samples quenched from a temperature close to the liquidus temperature revealed a refined microstructure at a high amount of Ti and C. This result indicates that the nucleation process is strongly activated with an increasing Ti and C amount in the detriment of the growth process which dominates at a low amount of Ti and C.

The electromagnetic levitation technique has been used in order to investigate the influence of melt rotation on the microstructure formation of Nd-Fe-B alloys mainly

the volume fraction of the α -Fe phase and the grain size. Samples were subjected to strong rotation during levitation and compared with fixed samples without additional (to the internal melt convection) sample rotation in the levitation facility. The determination of the α -Fe volume fraction by measuring the magnetic moment in a vibrating sample magnetometer (VSM) resulted in a drastic reduction of the α -Fe volume fraction in samples with strong sample rotation.

The solidification process and the resulting microstructure of Nd-Fe-B alloys in consideration of melt convection has been investigated experimentally with a specially designed forced crucible rotation technique. It was deduced from numerical simulation of fluid flow that compared to the non-rotating case, the global melt rotation suppresses the internal melt motion significantly by about two orders of magnitude. The experiments with different rotation frequencies resulted in a strong reduction of the soft magnetic α -Fe phase at reduced internal melt motion corresponding to increasing global crucible rotation. Moreover, experiments with strong enhanced internal melt motion carried out with a sample shaking procedure confirmed the results.

Furthermore, a new category of experiment has been started where a tailored magnetic field was applied in order to study the microstructure evolution due to a forced enhancement or suppression of the melt convection by additional alternating magnetic fields.

References

- [1] M. Sagawa, S. Fujimura, N. Togawa, H. Yamamoto, Y. Matura, *J. Appl. Phys.* **55**, 2083 (1984).
- [2] E. Schleich, R. Willnecker, D. M. Herlach, G. P. Görlner, *Mater. Sci. Eng.* **98**, 39 (1988).
- [3] R. Hermann, I. Baecher, W. Loeser, L. Schultz, *J. Magn. Magn. Mater.* **197**, 737 (1999).
- [4] R. Hermann, I. Baecher, *J. Magn. Magn. Mater.* **213**, 82 (2000).
- [5] R. Hermann, O. Filip, N. Matern, L. Schultz, *Proc. 16-th International Workshop on Rare-earth Magnets and their Applications*, Sendai, Japan, 2000.
- [6] T. Kozuka, M. Kawahara, *Proc. of the Third International Symposium on Electromagnetic processing of Materials*, Nagoya, Japan, 2000, p. 519.
- [7] R. Hermann, O. Filip, *J. Magn. Magn. Mater.* **263**, 15 (2003).
- [8] O. Filip, R. Hermann, L. Schultz, *J. Magn. Magn. Mater.* **234**, 247 (2001).
- [9] R. Hermann, W. Löser, *J. Appl. Phys.* **83**, 6399 (1998).
- [10] V. Shatrov, J. Priede, G. Gerbeth, *Phys. Fluids* **15**(3), 668 (2003).
- [11] R. Hermann, G. Behr, G. Gerbeth, J. Priede, H.-J. Uhlemann, F. Fischer, L. Schultz, *J. Crystal Growth* **275**(1-2), e1533-e1538 (2005).

*Corresponding author: octavian.filip@ww.uni-erlangen.de